Inverse Problems in Astrophysics

•Part 1: Introduction inverse problems and image deconvolution

•Part 2: Introduction to Sparsity and Compressed Sensing

•Part 3: Wavelets in Astronomy: from orthogonal wavelets and to the Starlet transform.

•Part 4: Beyond Wavelets

•Part 5: Inverse problems and their solution using sparsity: denoising, deconvolution, inpainting, blind source separation.

•Part 6: CMB & Sparsity

•Part 7: Perspective of Sparsity & Compressed Sensing in Astrophsyics

INVERSE PROBLEMS AND SPARSE RECOVERY

$$Y = HX + N$$

$X = \Phi\alpha$, and α is sparse

- **Denoising**
- **Deconvolution**
- **Component Separation**
- **Inpainting**
- **Blind Source Separation**
- **Minimization algorithms**
- **Compressed Sensing**

$$\min_{\alpha} \|\alpha\|_p^p \quad \text{subject to} \quad \|Y - H\Phi\alpha\|^2 \leq \epsilon$$

Very efficient recent methods now exist to solve it (proximal theory)

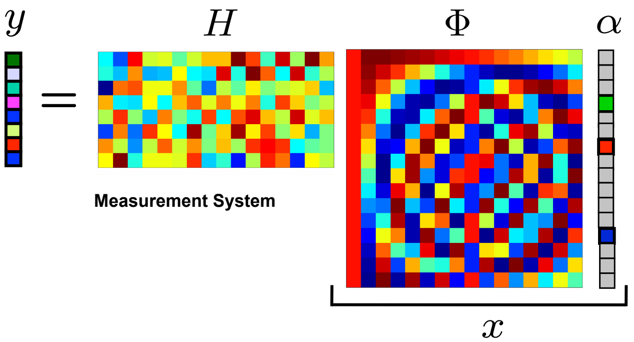

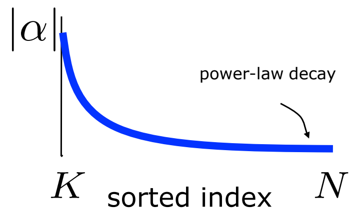

$$Y = HX + N$$

Between all possible solutions, we want the one which has the sparsest representation in the dictionary Φ. It leads to the following optimization problem:

$$\min_{\alpha_1,\cdots,\alpha_T} \frac{1}{2\sigma^2} \|Y - H\Phi\alpha\|^2 + \lambda \sum_{i=1}^{T} \|\alpha_i\|_p^p \ , 0 \leq p < 2 \ .$$

$$X = \Phi\alpha$$

A sparse model can be interpreted in a Bayesian framework

Assuming the coefficients α of the solution in the dictionary Φ follow a leptokurtic PDF with heavy tails such as the generalized Gaussian distribution form:

$$\mathrm{pdf}_\alpha(\alpha_1,\ldots,\alpha_T) \propto \prod_{i=1}^{T} \exp\left(-\lambda \|\alpha_i\|_p^p\right) \quad 0 \leq p < 2 \ .$$

Denoising using a sparsity model

Denoising using a sparsity prior on the solution:

X is sparse in Φ, i.e. $X = \Phi\alpha$ where most of α are negligible.

$$\tilde{\alpha} \in \arg\min_{\alpha} \frac{1}{2} \parallel Y - \Phi\alpha \parallel^2 + t \parallel \alpha \parallel_p^p, \quad 0 \leq p \leq 1.$$

P=0

$$\tilde{\alpha} \in \arg\min_{\alpha} \frac{1}{2} \parallel Y - \Phi\alpha \parallel^2 + \frac{t^2}{2} \parallel \alpha \parallel_0$$

==> Solution via Iterative **Hard** Thresholding

$$\tilde{\alpha}^{(t+1)} = \mathrm{HardThresh}_{\mu t}(\tilde{\alpha}^{(t)} + \mu\Phi^T(Y - \Phi\tilde{\alpha}^{(t)})), \mu = 1/\left\|\Phi\right\|^2.$$

$$\tilde{\alpha}_{j,k} = \mathrm{HardThresh}_t(\alpha_{j,k}) = \begin{cases} \alpha_{j,k} & \text{if } \mid \alpha_{j,k} \mid \geq t, \\ 0 & \text{otherwise.} \end{cases}$$

1st iteration solution:

$$\tilde{X} = \Phi\ \mathrm{HardThresh}_t(\Phi^T Y) = \Delta_{\Phi,t}(Y)$$

Exact for Φ orthonormal.

Detection in the Wavelet Domain

NOISE MODELING

For a positive coefficient: $P = \Pr ob(w > w_{j,x,y})$

For a negative coefficient: $P = \Pr ob(w < w_{j,x,y})$

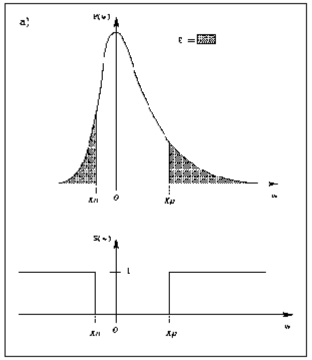

Given a threshold t:

if P > t, the coefficient could be due to the noise.

if P < t, the coefficient cannot be due to the noise, and a **significant coefficient** is detected.

Noise Modeling in the wavelet space

The noise in the data follows a distribution law which can be:

- a White Gaussian Noise
- Correlated Noise
- a Poisson Noise
- a Poisson + Gaussian distribution (noise in the CCD)
- Poisson noise with few events (Galaxies counting, X ray images, ...)
- Speckle noise
- Root Mean Square map: we have a noise standard deviation of each data value.

Gaussian Noise

$$p(w_{j,l}) = \frac{1}{\sqrt{2\pi}\sigma_j} e^{-w_{j,l}^2/2\sigma_j^2}$$

Rejection of hypothesis $\mathcal{H}$, depends (for a positive coefficient value) on:

$$P = Prob(w_{j,l} > W) = \frac{1}{\sqrt{2\pi}\sigma_j} \int_{w_{j,l}}^{+\infty} e^{-W^2/2\sigma_j^2} dW$$

and if the coefficient value is negative, it depends on

$$P = Prob(w_{j,l} < W) = \frac{1}{\sqrt{2\pi}\sigma_j} \int_{-\infty}^{w_{j,l}} e^{-W^2/2\sigma_j^2} dW$$

Given stationary Gaussian noise, it suffices to compare $w_{j,l}$ to $k\sigma_j$.

if $\mid w_j \mid \geq \ k\sigma_j$ then w_j is significant

if $\mid w_j \mid < \ k\sigma_j$ then w_j is not significant

Threshold estimation: Gaussian case

1. k-sigma: $$T_j = k\sigma_j$$

2. Universal Threshold: $$T_j = \sqrt{2\log n}\sigma_j$$

3. False Discovery Rate (FDR): compute the p-values for each wavelet coefficient $w_{j,l}$ at scale j and position l using the noise level σ_j. <u>The user parameter α determines **the number of false detections as a percentage of the number of true detections. The FDR fixes the threshold.**</u>

Poisson Noise

If the noise in the signal s is Poisson, the transform

$$t(s_k) = 2\sqrt{s_k + \frac{3}{8}}$$

acts as if the data arose from a Gaussian white noise model (Anscombe, 1948), with $\sigma = 1$, under the assumption that the mean value of I is large.

Poisson Noise + Gaussian

The generalization of the variance stabilizing is:

$$t(s_k) = \frac{2}{\alpha}\sqrt{\alpha s_k + \frac{3}{8}\alpha^2 + \sigma^2 - \alpha g}$$

where α is the gain of the detector, and g and σ are the mean and the standard deviation of the read-out noise.

Sparsity - Haar Wavelets for Poisson denoising

$$\Phi = \{\phi_1, \ldots, \phi_K\}$$

$$s = \sum_{k=1}^{K} \alpha_k \phi_k = \Phi\alpha$$

$$f(x) = c_0 + \sum_{j=0}^{\infty} \sum_{k=0}^{2^j-1} c_{jk} \psi_{jk}(x).$$

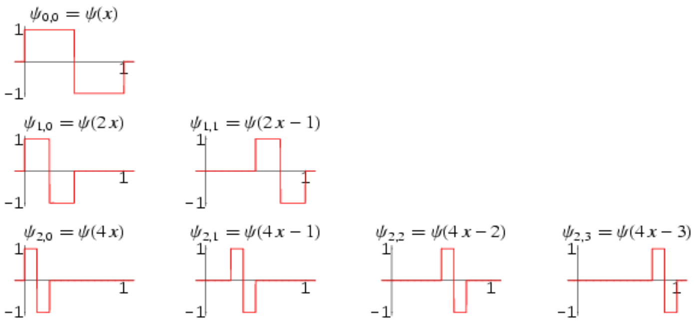

Kolaczyk: ApJ, 1997; Stat Sinica, 1999; ApJ, 2000.
Bijoui & Jammal: Signal Processing, 2001.
Willett: Statistical Challenges in Modern Astronomy (SCMA) IV, 2006.
P. Fryzˊlewicz and G. P. Nason: J. Roy. Stat. Soc., 2007.
Zhang, Fadili, Starck, Digel: Statistical Methodology, 2008.

Multiscale Variance Stabilization

$$\text{IUWT} \quad \begin{cases} a_j &= \bar{h}^{\uparrow j-1} \star a_{j-1} \\ w_j &= a_{j-1} - a_j \end{cases}$$

$$\Longrightarrow \quad \begin{matrix}\text{MSVST} \\ + \\ \text{IUWT}\end{matrix} \quad \begin{cases} a_j &= \bar{h}^{\uparrow j-1} \star a_{j-1} \\ w_j &= \mathcal{A}_{j-1}(a_{j-1}) - \mathcal{A}_j(a_j) \end{cases}$$

$$\mathcal{A}_j(a_j) = b^{(j)} \sqrt{a_j + c^{(j)}}$$

$$c^{(j)} = \frac{7\tau_2^{(j)}}{8\tau_1^{(j)}} - \frac{\tau_3^{(j)}}{2\tau_2^{(j)}} \quad , \quad b^{(j)} = 2\sqrt{\frac{\tau_1^{(j)}}{\tau_2^{(j)}}}$$

$$\tau_k^{(j)} = \sum_i \left(h^{(j)}[i]\right)^k$$

ISOTROPIC UNDECIMATED WAVELET TRANSFORM

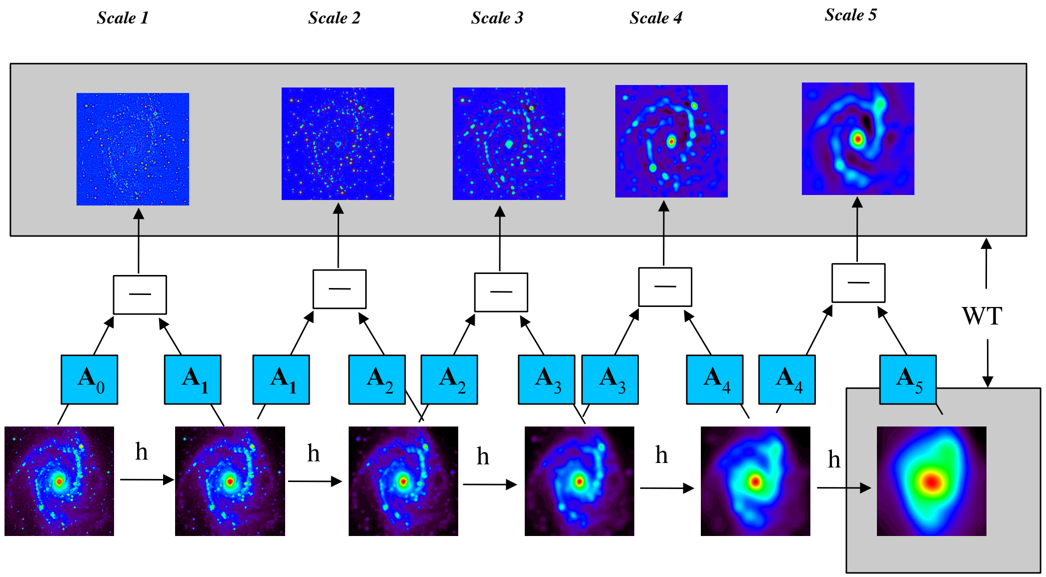

J.-L. Starck, M.J. Fadili, S. Digel , B. Zhang and J. Chiang, "Source Detection Using a 3D Sparse Representation: Application to the Fermi Gamma-ray Space Telescope ", Astronomy and Astrophysics , 504, 2, pp.641-652, 2009.

J. Schmitt, J.L. Starck, J.M. Casandjian, M.J. Fadili, I. Grenier, "Poisson Denoising on the Sphere: Application to the Fermi Gamma Ray Space Telescope", Astronomy and Astrophysics, 517, A26, 2010.

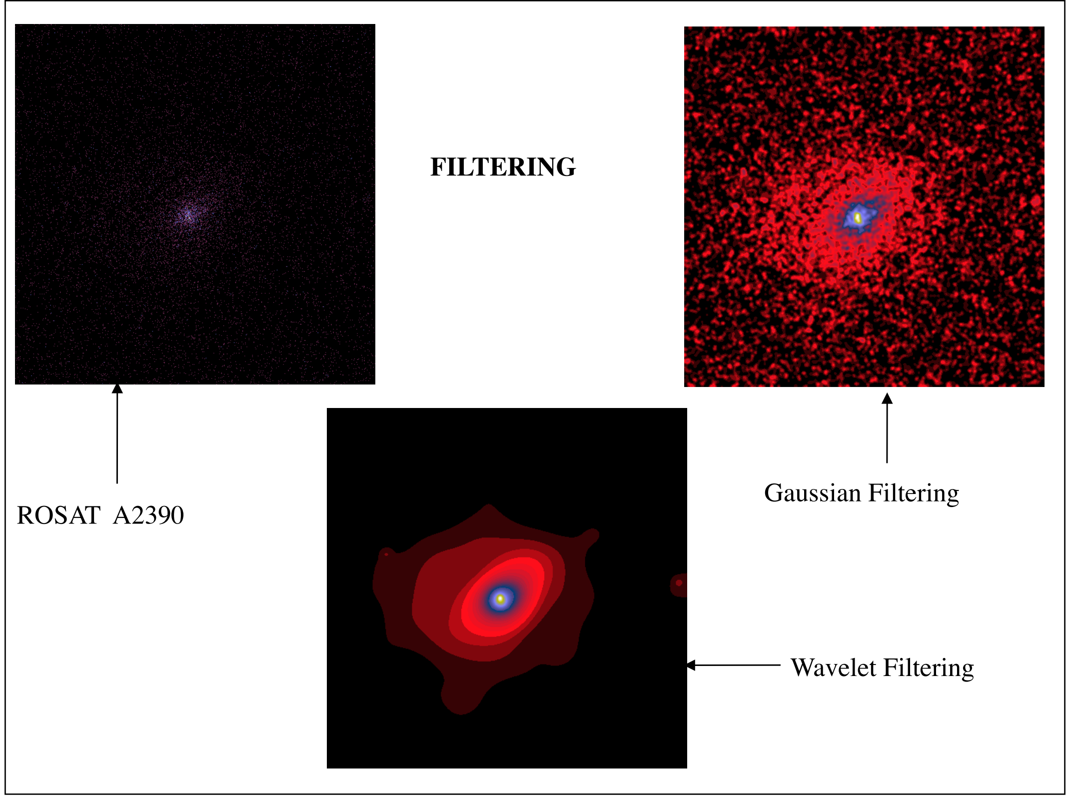
FILTERING
ROSAT A2390
Gaussian Filtering
Wavelet Filtering

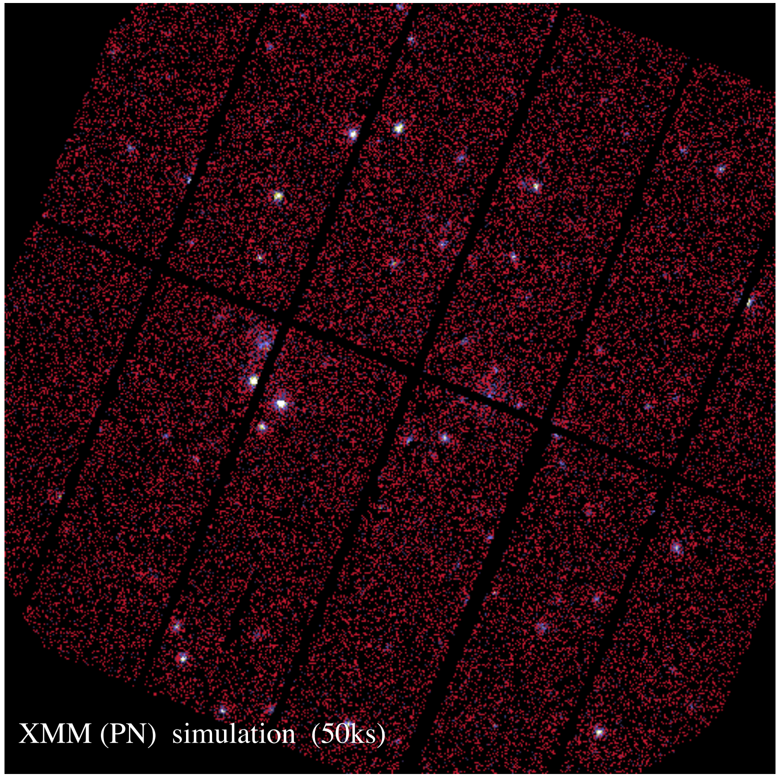
XMM (PN) simulation (50ks)

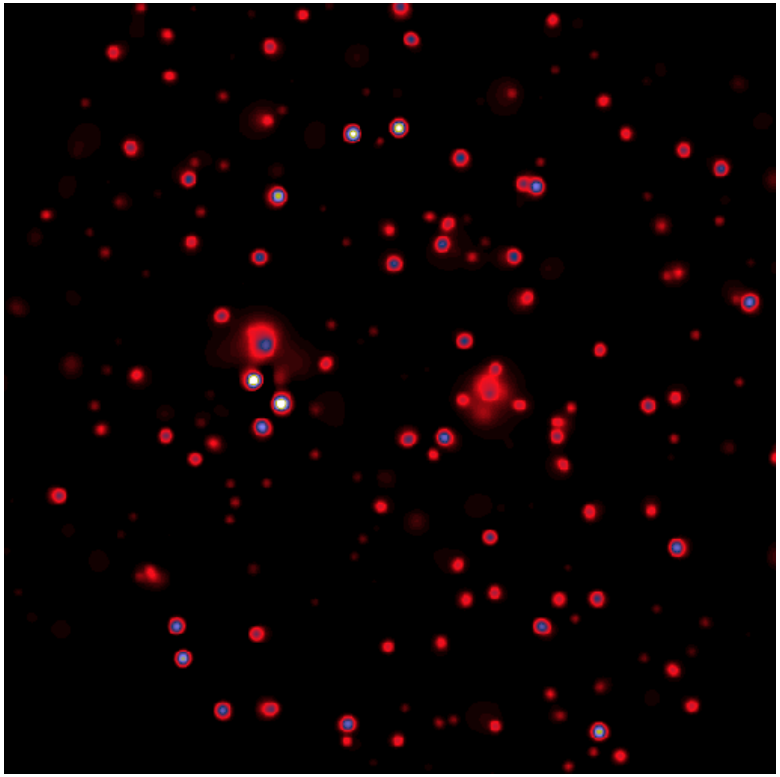

Inverse Problems and Iterative Thresholding Minimizing Algorithm

Iterative thresholding with a varying threshold was proposed in (Starck et al, 2004; Elad et al, 2005) for sparse signal decomposition in order to accelerate the convergence. The idea consists in using a different threshold $\lambda^{(n)}$ at each iteration.

$$\alpha^{(n+1)} = \mathrm{HT}_{\lambda^{(n)}}\left(\alpha^{(n)} + \Phi^T H^T \left(Y - H\Phi\alpha^{(n)}\right)\right)$$

$$\alpha^{(n+1)} = \mathrm{ST}_{\lambda^{(n)}}\left(\alpha^{(n)} + \Phi^T H^T \left(Y - H\Phi\alpha^{(n)}\right)\right)$$

Refs: Vonesch et al, 2007; Elad et al 2008; Wright et al., 2008; Nesterov, 2008 and Beck-Teboulle, 2009; Blumensath, 2008; Maleki et Donoho, 2009, Starck et al, 2010, Raguet, Fadili, and Peyre, 2012; Vu , 2013 ; etc.

Analysis versus Synthesis Formulation

Analysis: $$\min_x \|Y - HX\|^2 + \lambda \|\Phi^t x\|_p^p$$

Synthesis: $$\min_\alpha \|Y - H\Phi\alpha\|^2 + \lambda \|\alpha\|_p^p$$

Analysis framework generally gives better results than the synthesis framework.

l_0 norm generally gives better results than l_1 norm.

Multiple thresholds

$$Y = HX + N \qquad X = \Phi\alpha \text{ and } \alpha \text{ is sparse}$$

Analysis: $\min_x \|Y - HX\|^2 + \lambda \|\Phi^t x\|_p^p$

Synthesis: $\min_\alpha \|Y - H\Phi\alpha\|^2 + \lambda \|\alpha\|_p^p$

The use of a single hyper parameter does not allow us to properly take into account the signal and noise behavior in different bands:

$$\min_x \|Y - HX\|^2 + \sum_j \lambda_j \|\Phi_j^t x\|_p^p$$

$$\min_\alpha \|Y - H\Phi\alpha\|^2 + \sum_j \lambda_j \|\alpha_j\|_p^p$$

Signal driven strategy

Study the statistical distribution of the coefficient of a class of signal in the different bands (amplitude, decay, etc).

Noise driven strategy from MC noise realizations

$$\alpha_j^{N^{(i)}} = \Phi_j^t H^T N^{(i)} \quad \text{and} \quad \lambda_j = k\sigma(\alpha_j^{N^{(i)}})$$

Spatially variant noise

$$\alpha^{R^{(n)}} = \Phi^t H^T \left(Y - Hx^{(n)}\right)$$

$$\alpha_{j,l}^{N^{(i)}} = \left(\Phi_j^t H^T N^{(i)}\right)_l \qquad \lambda_{j,l} = k\sigma\left(\alpha_{j,l}^{N^{(i)}}\right)$$

Noise driven strategy from the residual

$$\alpha^{R^{(n)}} = \Phi^t H^T \left(Y - Hx^{(n)}\right) \qquad \lambda_j = k\sigma(\alpha_j^{R^{(n)}})$$

but no convergence prove anymore ....

The Moreau Proximal Operator

Moreau (1962) introduced the notion of **proximity operator** as a generalization of a convex projection operator.

The function $\frac{1}{2}\|y - x\|^2 + \mathcal{C}(x)$ achieves its minimum at a unique point denoted by $\mathrm{prox}_{\mathcal{C}}(x)$.

The operator $\mathrm{prox}_{\mathcal{C}}$ is the proximity operator of $\mathcal{C}$.

$$\mathcal{C}(x) = \frac{1}{2}\lambda\|x\|^2 \rightarrow \mathrm{prox}_{\mathcal{C}}(x) = \frac{x}{1+\lambda}.$$

$$\mathcal{C}(x) = \lambda\|x\|_1 \rightarrow \mathrm{prox}_{\mathcal{C}}(x) = \mathrm{SoftThreshold}_{\lambda}(x) = \mathrm{sgn}(x)\mathrm{max}(|x| - \lambda, 0).$$

Euclidian projection on convex set Ω

The indicator function of a closed convex subset Ω is the function defined

$$1_{\Omega}(\mathbf{x}) = \begin{cases} 0, & \text{if } \mathbf{x} \in \Omega \\ +\infty, & \text{otherwise.} \end{cases}$$

The proximity operator of $1_{\mathcal{C}}$ is the orthogonal projector onto Ω.

Forward-Backward Algorithm

$$\min_{\alpha} \|Y - H\Phi\alpha\|^2 + \lambda\|\alpha\|_p^p$$

Iterative Soft Threshold Algorithm (IST)

$$\alpha^{n+1} = \mathrm{prox}_{\Phi,\lambda}(\alpha^n + \mu\Phi^t H^t (Y - H\Phi\alpha^n)).$$

IST can be seen as a generalization of projected gradient descent.

Drawback: slow convergence, O(1/n)

FISTA

[Beck, Teboulle, 2009]

$$\mathrm{t}^{n+1} = \frac{1+\sqrt{1+4(t^n)^2}}{2}$$

$$z^{n+1} = \alpha^n + \frac{t^n - 1}{t^n + 1}(\alpha^n - \alpha^{n-1})$$

$$\alpha^{n+1} = \mathrm{prox}_{\mu\lambda}(z^{n+1} + \mu\Phi^t H^t (y - H\Phi\alpha^n))$$

convergence, $O(\frac{1}{n^2})$

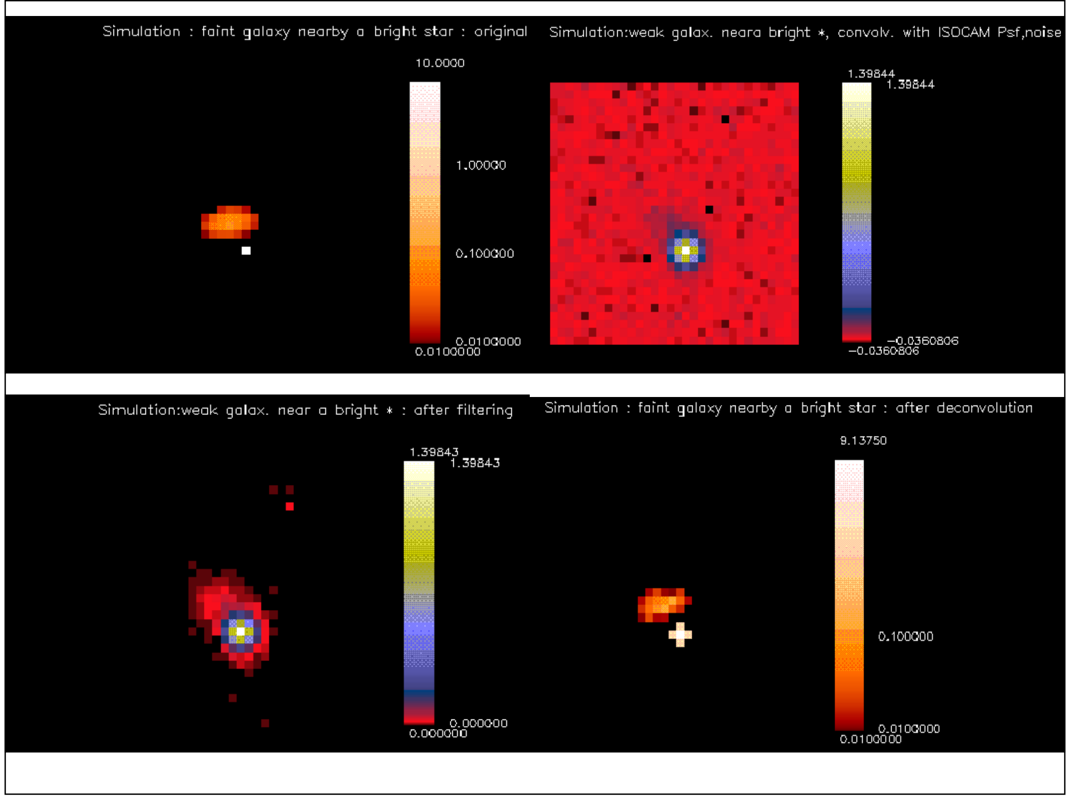

Simulation : faint galaxy nearby a bright star : original
10.0000
1.00000
0.100000
0.0100000
0.0100000
Simulation:weak galax. neara bright *, convolv. with ISOCAM Psf,noise
1.39844
1.39844
-0.0360806
-0.0360806
Simulation:weak galax. near a bright * : after filtering
1.39843
1.39843
0.000000
0.000000
Simulation : faint galaxy nearby a bright star : after deconvolution
9.13750
0.100000
0.0100000
0.0100000

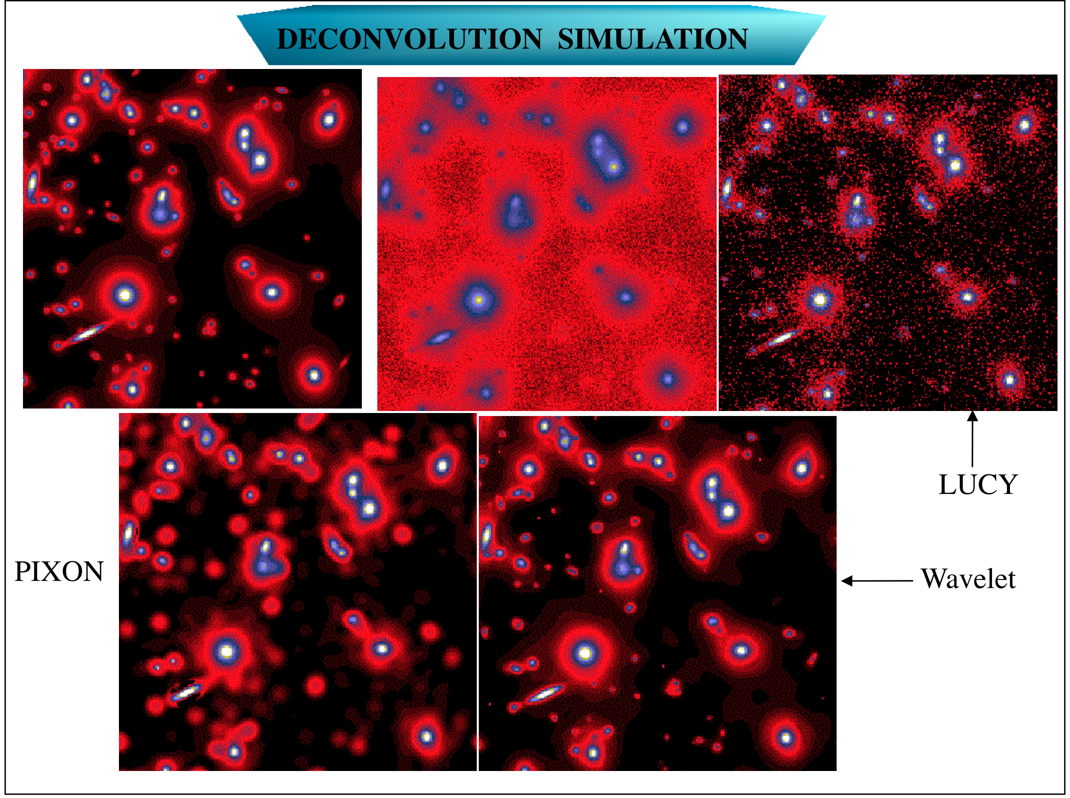
DECONVOLUTION SIMULATION
LUCY
PIXON
Wavelet

Radio-Interferometry Image Reconstruction

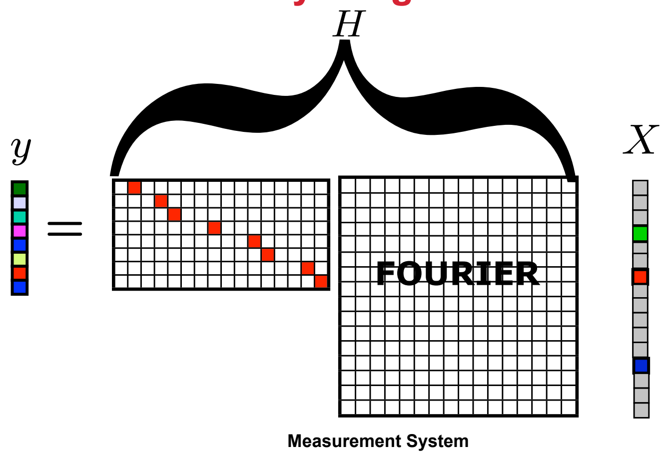

$$Y = HX + N$$

Compressed Sensing Theory and Radio-Interferometry

==> See (McEwen et al, 2011; Wenger et al, 2010; Wiaux et al, 2009; Cornwell et al, 2009; Suskimo, 2009; Feng et al, 2011; Garsden, Starck and Corbel, 2013).

Radio-Interferometry Sparse Recovery

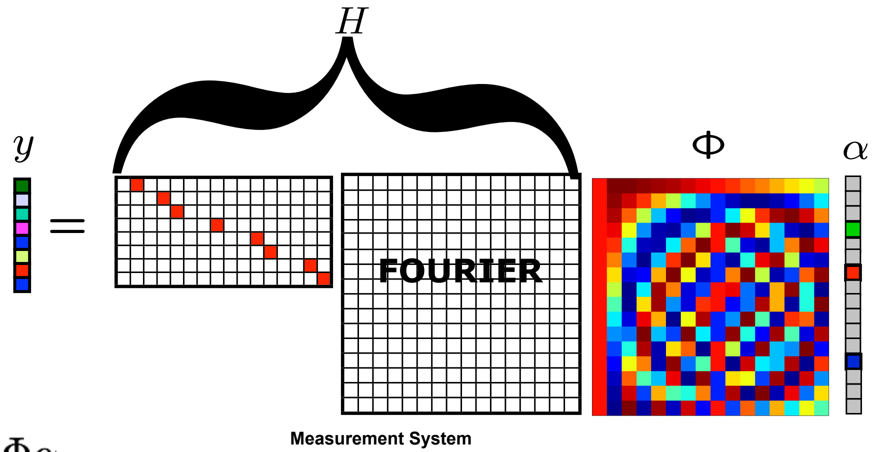

$$X = \Phi\alpha$$

$$\min_{\alpha} \|\alpha\|_p^p \quad \text{subject to} \quad \|Y - H\Phi\alpha\|^2 \leq \epsilon$$

- Garsden et al, "LOFAR Image Sparse Reconstruction", A&A, submitted. http://arxiv.org/abs/1406.7242

Sparse Recovery: Example

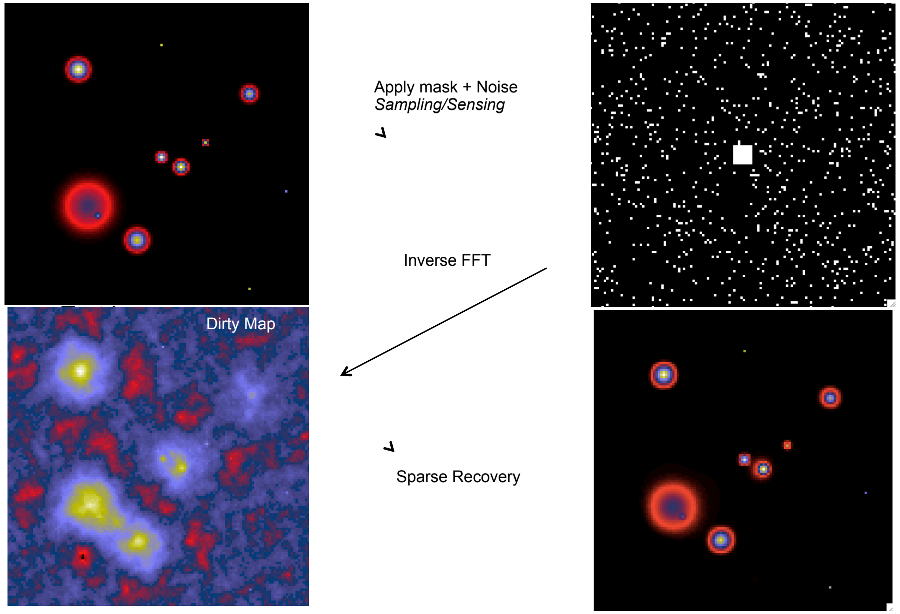

Experiment #1: Photometry

Simulated dataset

10x10 grid of
point sources

Random flux densities

[1-10000] Jy

Large field of view

8°x8°
centered at zenith

Widefield imaging

- CLEAN

- Sparse reconstruction

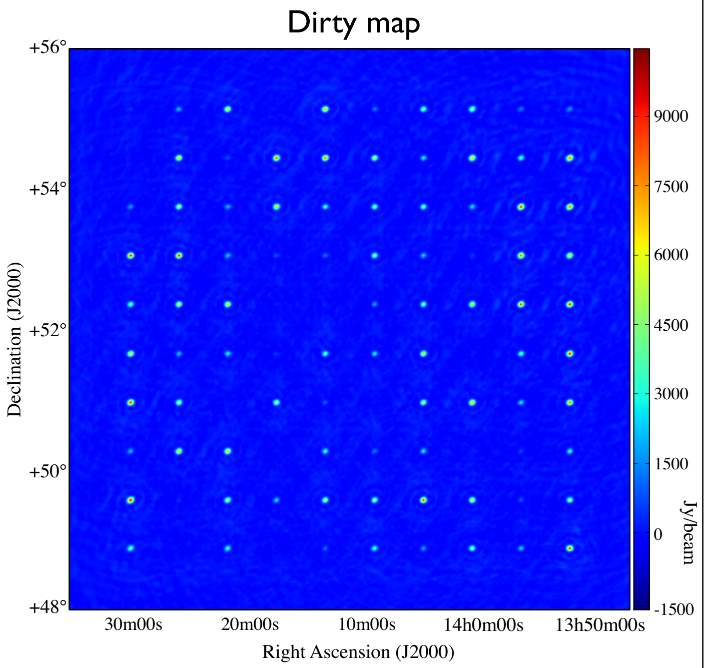

➢ recover flux densities from model images

Experiment #1: Photometry

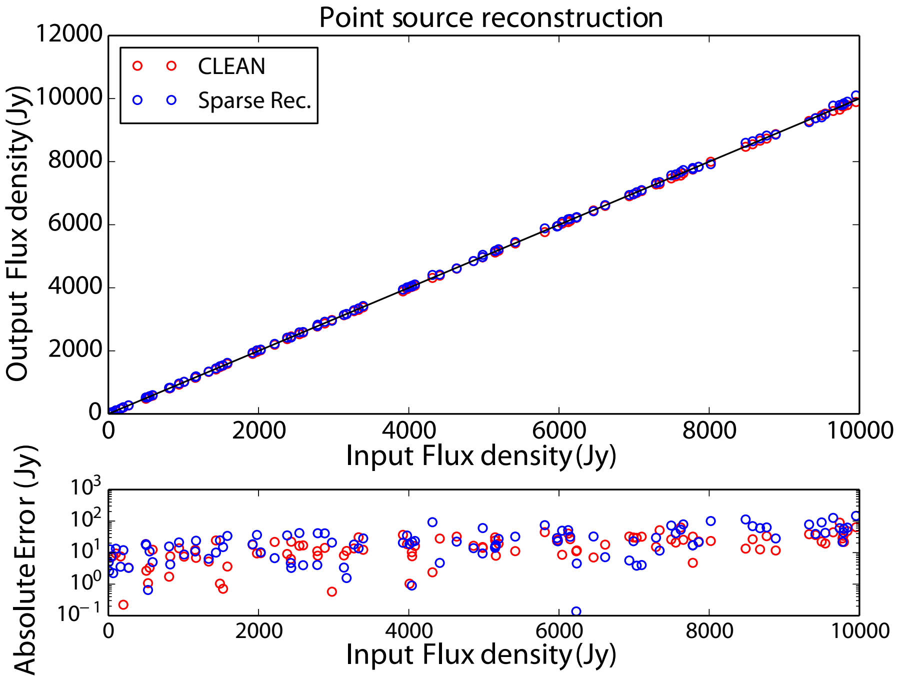

==> Sparse recovery provides similar results to CLEAN

Experiment #2: Angular separation

- Simulated LOFAR dataset

* Core stations only (N=24)

* ΔT=1h - ΔF=195 KHz - F=150 MHz

* Radial cut in the Fourier (u,v) plane at R_{uv}=1.6 kλ

➢ restricts artificially the resolution to ~2-3 arcminutes

- Filled with simulated data

* Two point sources of 1 Jy at zenith

* Source angular separation = from 10” to 5’

* Injected noise corresponding to SNR = 2.7, 8.9, 16 and 2000 (noiseless)

- Imaging with CLEAN and Sparse recovery

Experiment #1: Photometry

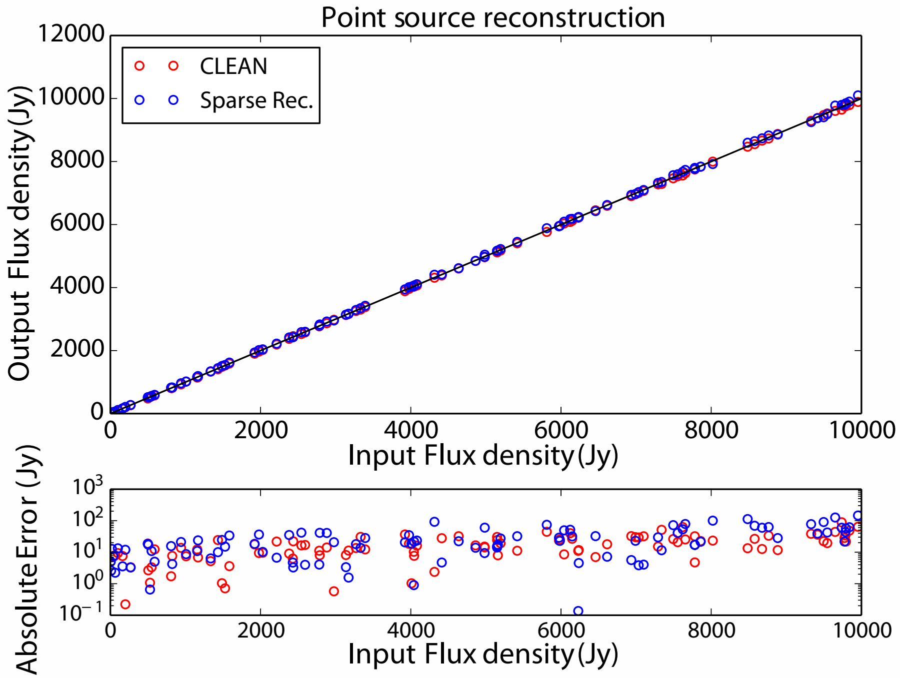

==> Sparse recovery provides **similar** results to CLEAN

Experiment #2: Angular separation

- Simulated LOFAR dataset

* Core stations only (N=24)

* $\Delta T=1h$ - $\Delta F=195$ KHz - F=150 MHz

* Radial cut in the Fourier (u,v) plane at $R_{uv}=1.6\ k\lambda$

➢ restricts artificially the resolution to ~2-3 arcminutes

- Filled with simulated data

* Two point sources of 1 Jy at zenith

* Source angular separation = from 10” to 5’

* Injected noise corresponding to SNR = 2.7, 8.9, 16 and 2000 (noiseless)

- Imaging with CLEAN and Sparse recovery

Experiment #2: Angular separation

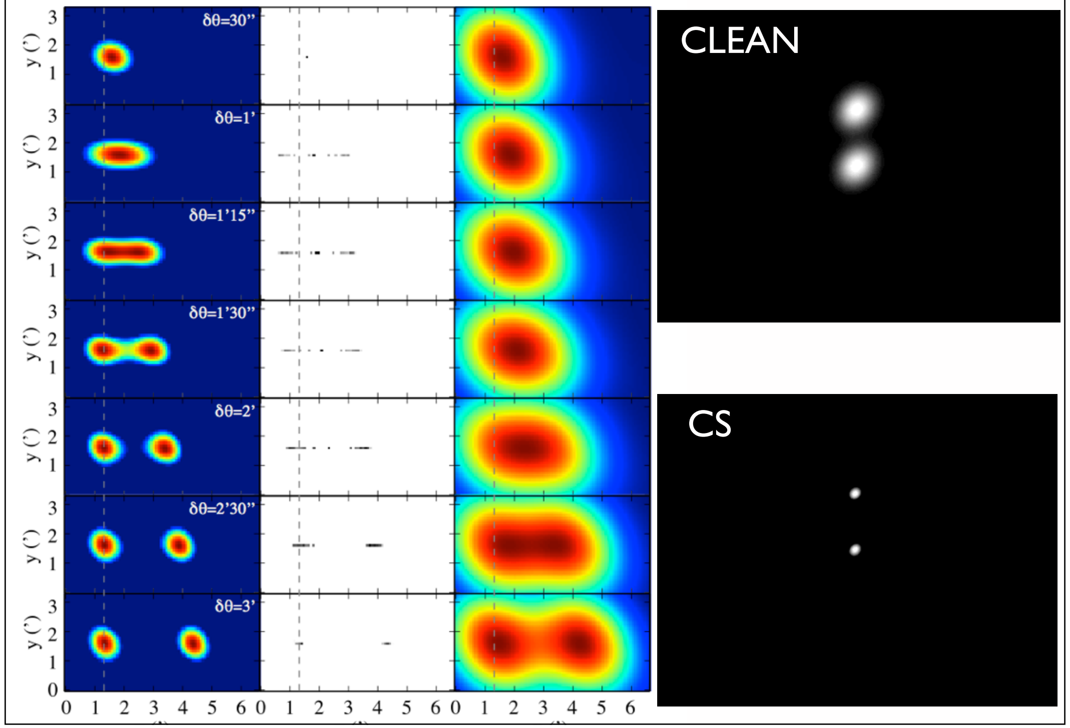

Experiment #2: Angular separation

Noiseless data

CLEAN

CLEAN beam = 3.2'x2.5'

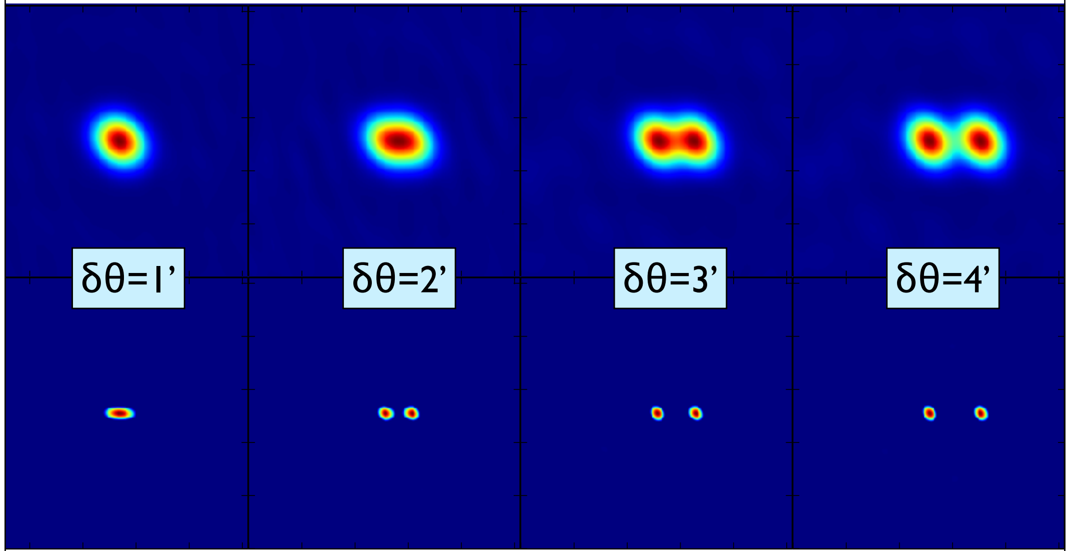

Sparse recovery

- Sparse Recovery resolution improved by at least 2 compared the CLEAN beam.
- Recovered « sub-beam » sources have correct fluxes (~2% error) & positions

Experiment #2: Angular separation

- On noisy data ➢ (rough) measurement of the source separability angle.

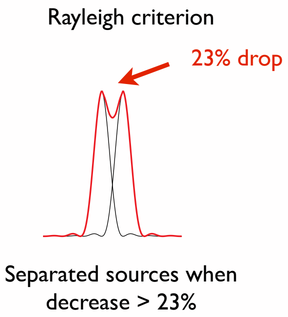

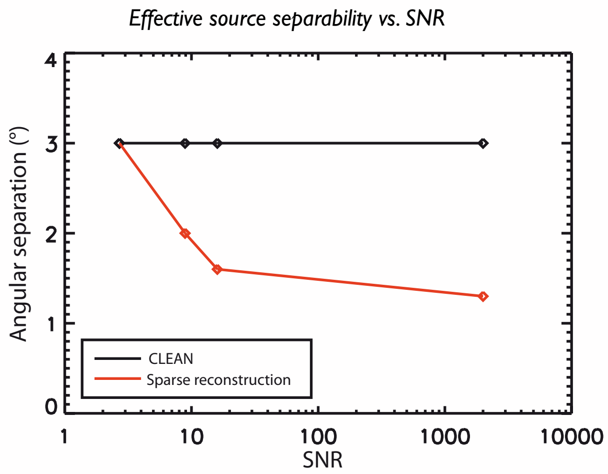

==> Sparse reconstruction: angular separation **improved by 2 for SNR > 10**, and converges to CLEAN resolution at low SNR regimes.

Experiment #3: Extended source

- VLA 21-cm image of W50 + empty simulated LOFAR dataset
- Set to an arbitrary flux scale and converted to visibilities (AWimager)

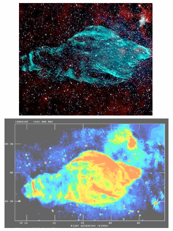

VLA @ 21 cm

Model image

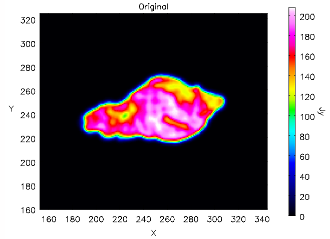

FFT
+
(u,v) Sampling

(u,v) coverage

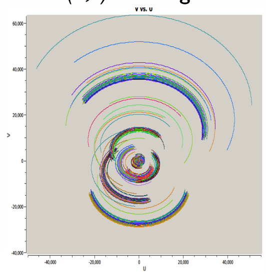

Dirty image

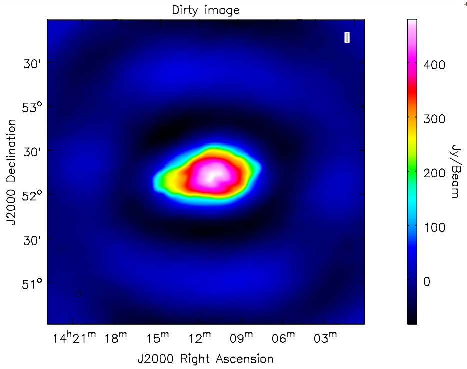

Experiment #3: Extended source

- Using CLEAN, Multiscale CLEAN and Sparse reconstruction

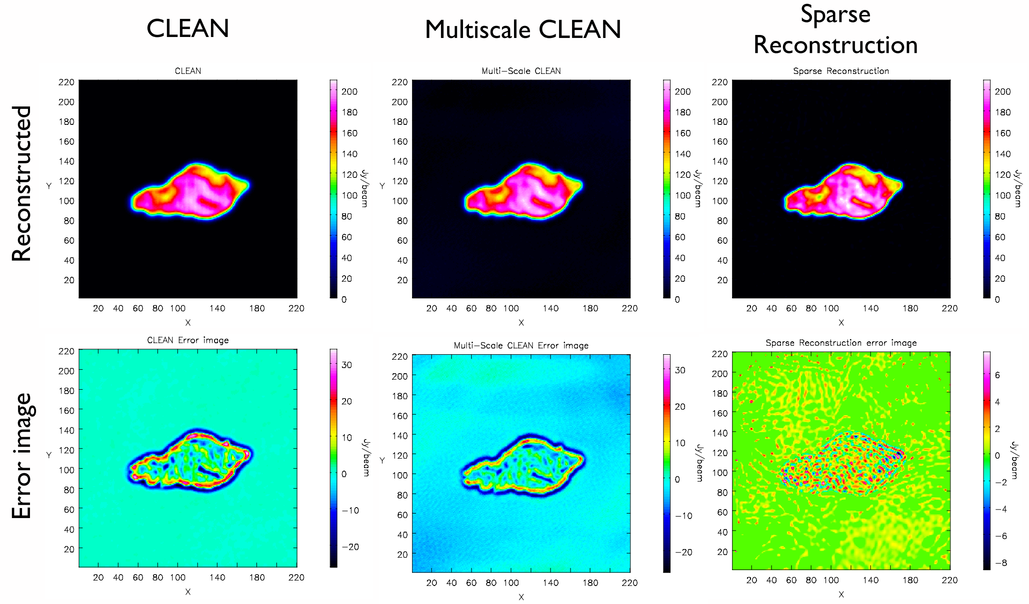

RMS error = 3.50

RMS error = 3.28

RMS error = 0.76

Experiment #3: Extended source

- Using CLEAN, Multiscale CLEAN and Sparse reconstruction

	CLEAN	Multiscale CLEAN	Sparse Reconstruction
Reconstructed			
Error image			

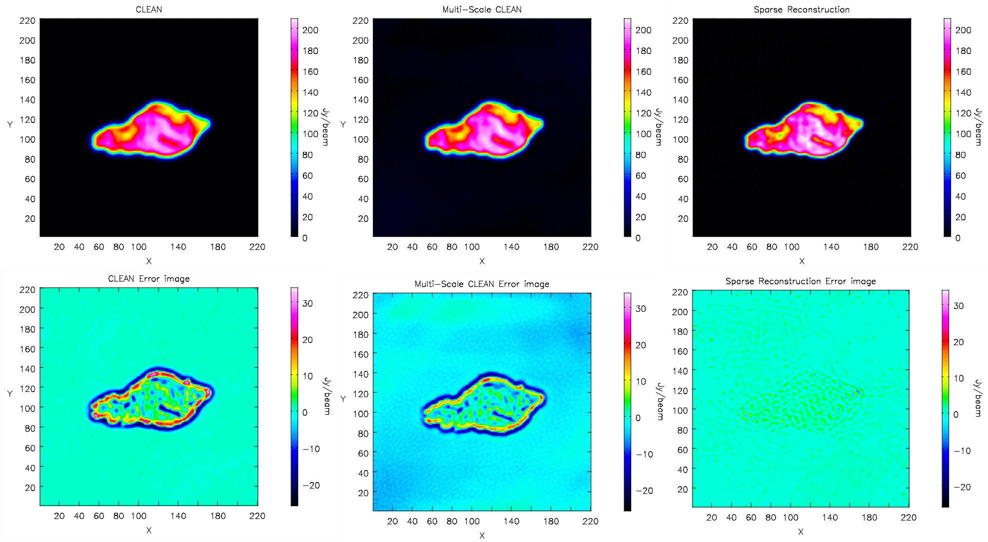

RMS error = 3.50	RMS error = 3.28	RMS error = 0.76

Experiment #4: Real data **Cygnus A**

F = 151 MHz - ΔF = 195 kHz

ΔT = 6 Hr

36 LOFAR Stations

(dataset courtesy of John Mckean)

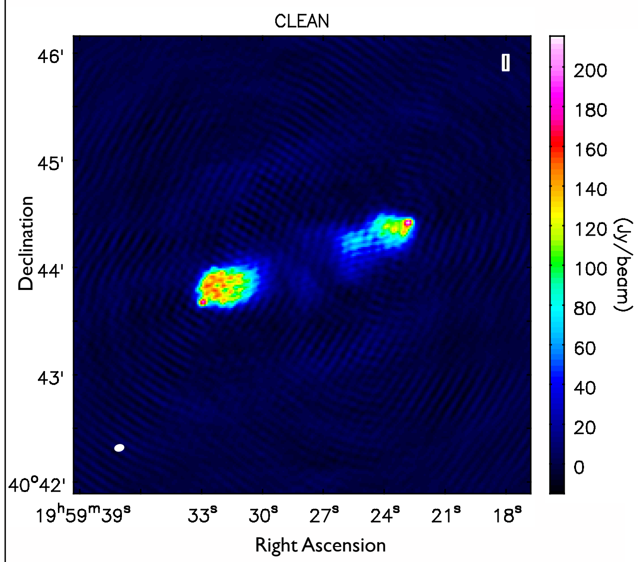

CLEAN

- Pixel = 1'' size = 512 x 512
- Threshold = 0.5 mJy
- Weighting = super uniform

Restored image

Total Flux density = 9393 Jy

Residuals

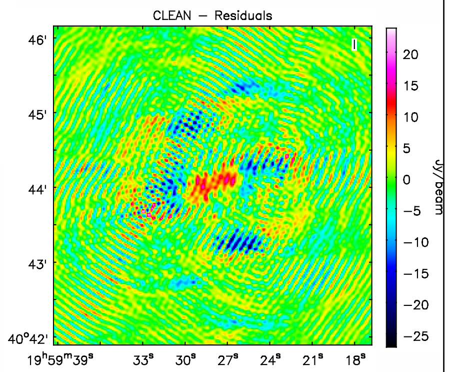

Residual std-dev = 2,65 Jy/beam

Cygnus A

F = 151 MHz - ΔF = 195 kHz

ΔT = 6 Hr

36 LOFAR Stations

(dataset courtesy of John Mckean)

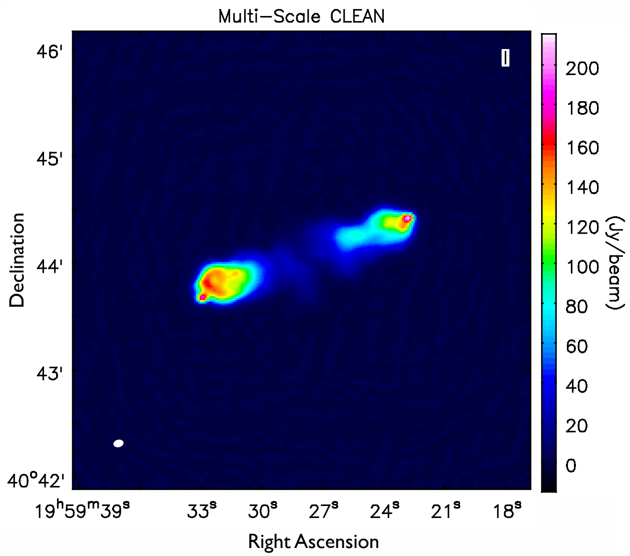

Multi-Scale CLEAN

- Pixel = 1'' size = 512 x 512
- Threshold = 0.5 mJy
- Weighting = super uniform
- Scales = [0, 5, 10, 15, 20] pixels

Restored image

Total Flux density = 10553 Jy

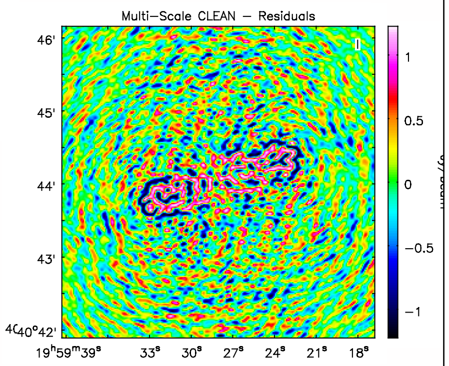

Residuals

Residual std-dev = 0,26 Jy/beam

Cygnus A

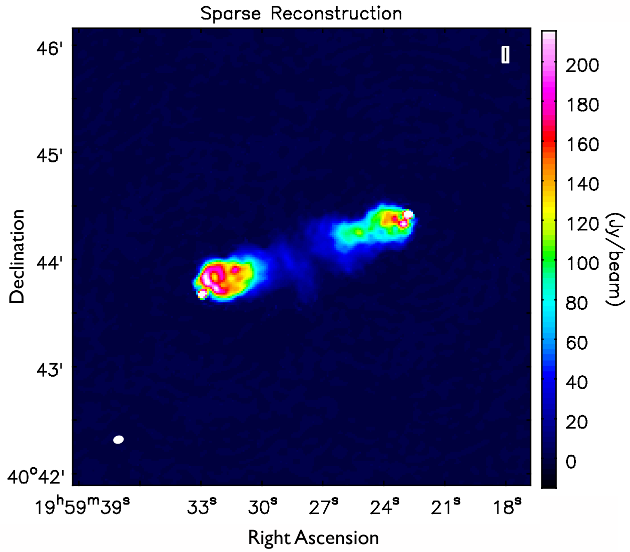

F = 151 MHz - ΔF = 195 kHz

ΔT = 6 Hr

36 LOFAR Stations

(dataset courtesy of John Mckean)

Sparse Reconstruction

- Pixel = 1'' size = 512 x 512
- Threshold = 0.5 mJy
- Weighting = super uniform
- Scales = 7 wavelets scales
- Minimization algorithm: FISTA

Fast Iterative Shrinkage-Thresholding Algorithm

Restored image

Total Flux density = 10506 Jy

Residuals

Residual std-dev = 0,05 Jy/beam

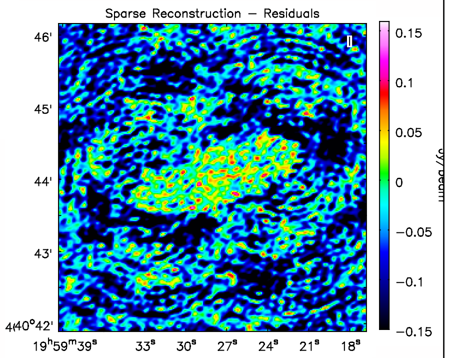

Reconstructed images of Cygnus A from the real LOFAR observations

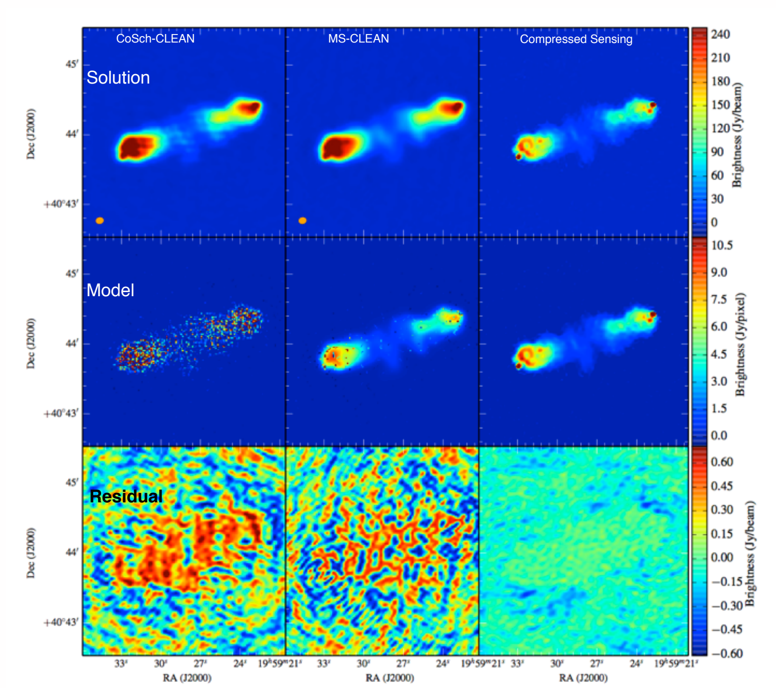

Residual std-dev = 2,65 Jy/beam, 0,26 Jy/beam, 0,05 Jy/beam

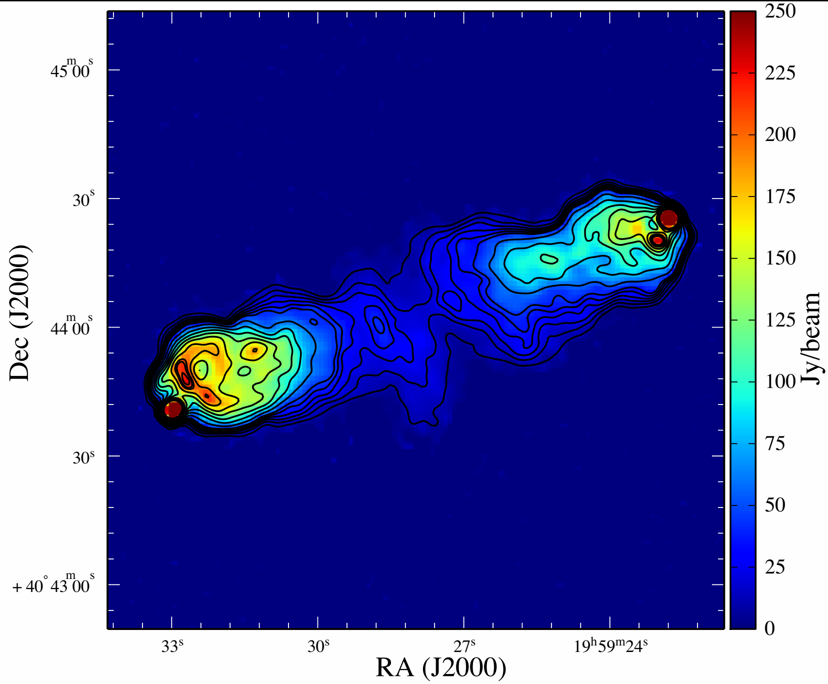

Colorscale: reconstructed 512x512 image of Cygnus A at 151 MHz (with resolution 2.8" and a pixel size of 1"). Contours levels are [1,2,3,4,5,6,9,13,17,21,25,30,35,37,40] Jy/Beam from a 327.5 MHz Cyg A VLA image (Project AK570) at 2.5" angular resolution and a pixel size of 0.5". Most of the recovered features in the CS image correspond to real structures observed at higher frequencies.

Period detection in temporal series

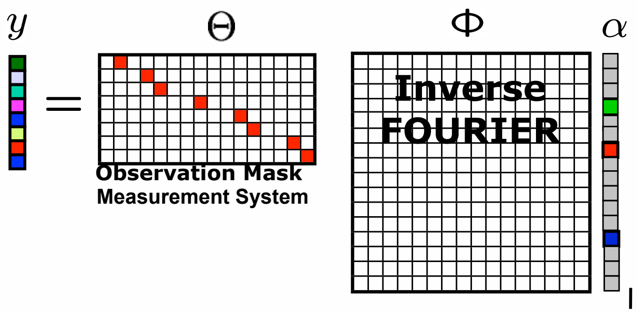

COROT: HD170987

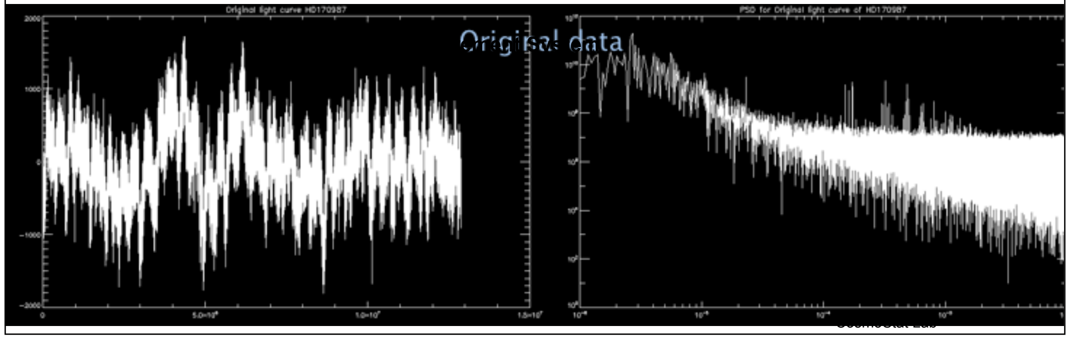

Inp  inting

- M. Elad, J.-L. Starck, D.L. Donoho, P. Querre, “Simultaneous Cartoon and Texture Image Inpainting using Morphological Component Analysis (MCA)", ACHA, Vol. 19, pp. 340-358, 2005.
- M.J. Fadili, J.-L. Starck and F. Murtagh, "Inpainting and Zooming using Sparse Representations", The Computer Journal, 52, 1, pp 64-79, 2009.

$$\min_{\alpha} \|\alpha\|_{\ell_0} \text{ s.t. } y = Mx$$

Where M is the mask: M(i,j) = 0 ==> missing data
M(i,j) = 1 ==> good data

$$x^{(n+1)} = \mathcal{S}_{\Phi,\lambda^{(n)}}\left\{x^{(n)} + M\left(y - x^{(n)}\right)\right\}$$

Iterative Hard Thresholding with a decreasing threshold.

MCAlab available at: http://www.greyc.ensicaen.fr/~jfadili

. Initialize all s_k to zero

. Iterate j=1,...,Niter

- Iterate k=1,..,L

  - Update the kth part of the current solution by fixing all other parts and minimizing:

$$J(s_k) = \left\| M\left(s - \sum_{i=1, i\neq k}^{L} s_i - s_k\right) \right\|_2^2 + \lambda \left\| T_k s_k \right\|_1$$

Which is obtained by a simple soft thresholding of :

$$s_r = M\left(s - \sum_{i=1, i\neq k}^{L} s_i\right)$$

COROT: HD170987 with in-painting

arXiv:1003.5178

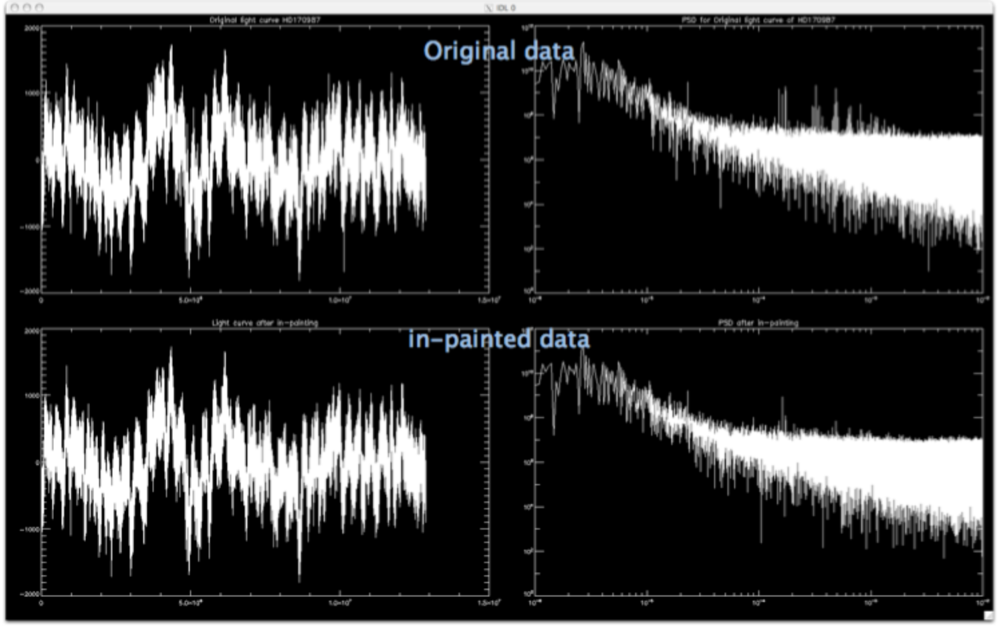

Sparse inpainting & asteroseismology

Gap interpolation by Inpainting methods: Application to Ground and Space-based data, S. Pires, S. Mathur, R.A. Garcia, J. Ballot, D. Stello and K. Sato, Astronomy and Astrophysics, submitted.

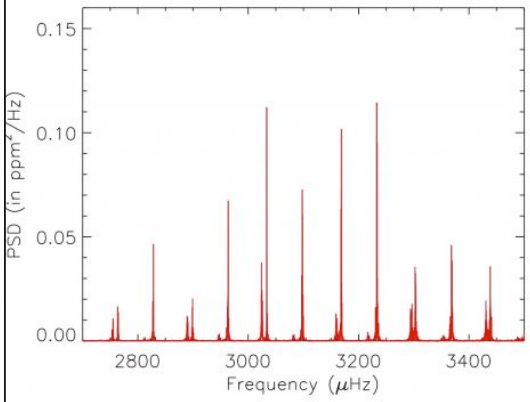

CoRo: sparse inpainting is in the official pipeline.
Kepler: 18.000 stars have been processed.
GOLF. ongoing tests

SOFTWARE K-INPAINTING : INPAINTING FOR KEPLER

S. Pires, R. A. Garcia, S. Mathur, J. Ballot www.cosmostat.org/software.html

http://irfu.cea.fr/Sap/en/Phocea/Vie_des_labos/Ast/ast_visu.php?id_ast=3346

20%

50%

80%

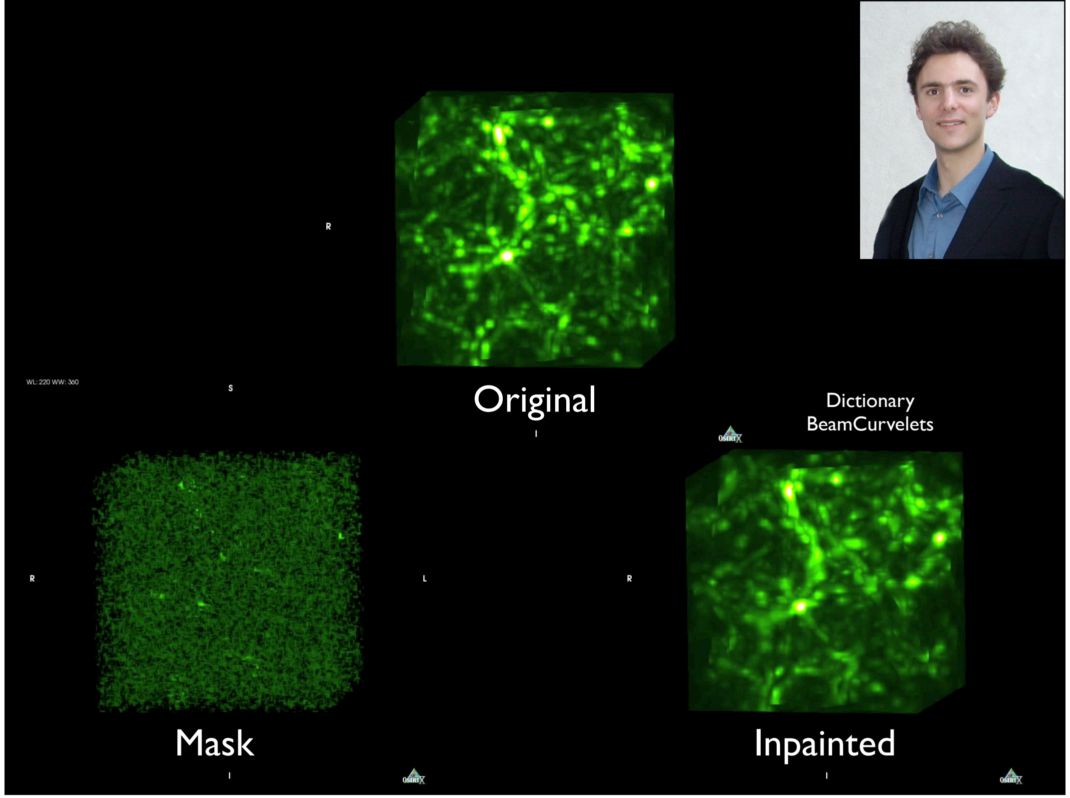
Original
Dictionary
BeamCurvelets
Mask
Inpainted

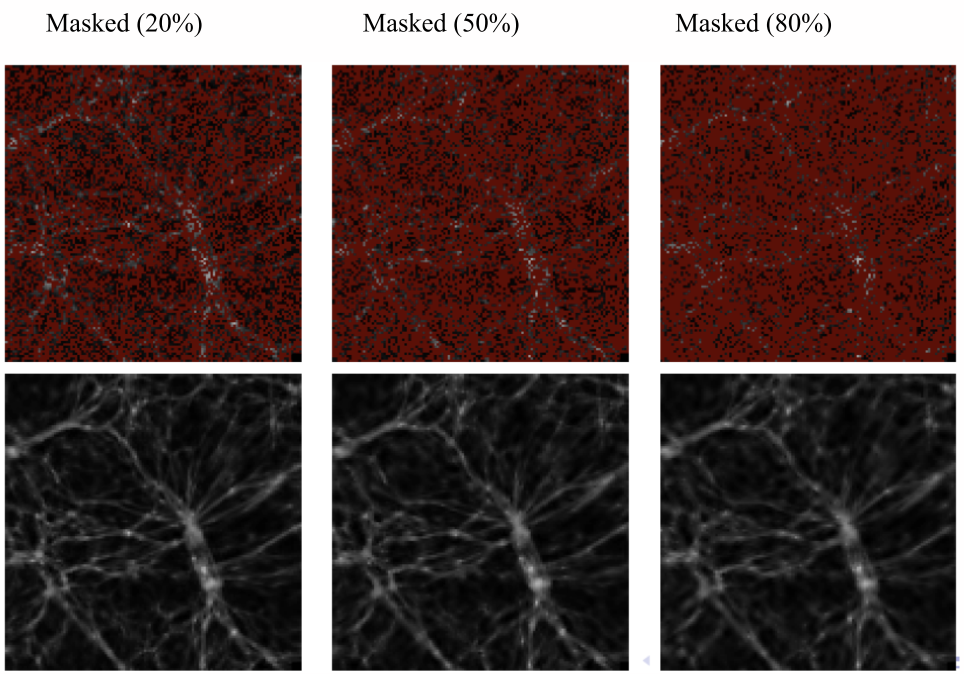

Central slice of the masked CDM data with 20, 50, and 80% missing voxels,
and the inpainted maps. The missing voxels are dark red.

Inpainting :

S. Pires, J.-L. Starck, A. Amara, R. Teyssier, A. Refregier and J. Fadili, "FASTLens (FAst STatistics for weak Lensing) : Fast method for Weak Lensing Statistics and map making", MNRAS, 395, 3, pp. 1265-1279, 2009.

Original map **Masked map** **Inpainted map**

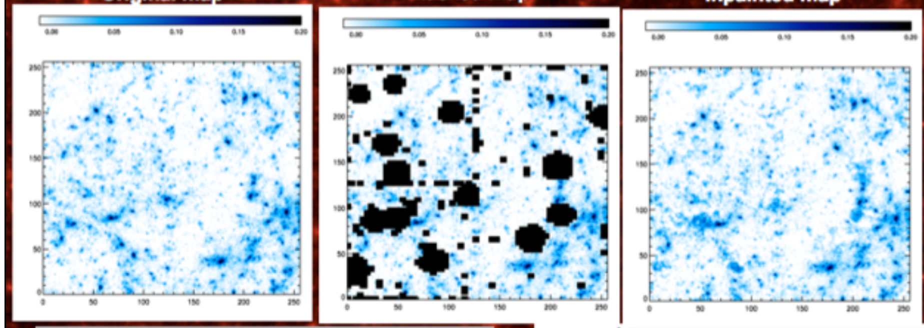

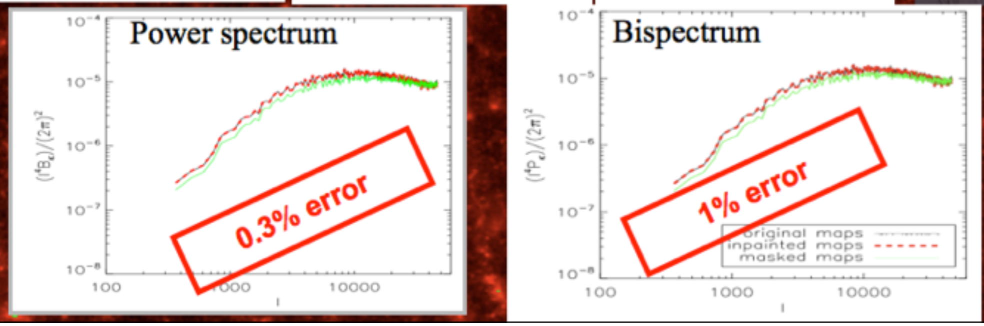

CMB & Sparse Inpainting

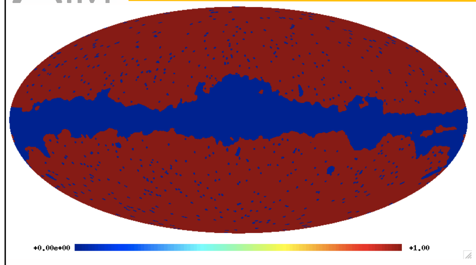

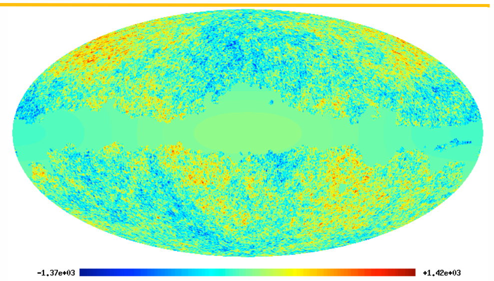

- Sparse-Inpainting preserves the weak lensing signal.

- L. Perotto, J. Bobin, S. Plaszczynski, J.-L. Starck, and A. Lavabre, "Reconstruction of the CMB lensing for Planck", *Astronomy and Astrophysics*, 2010.
- S. Plaszczynski, A. Lavabre, L. Perotto, J-L Starck, "An hybrid approach to CMB lensing reconstruction on all-sky intensity maps", arxiv.org/abs/1201.5779, *Astronomy and Astrophysics*, 544, A27, 2012.

- Sparse-Inpainting preserves the ISW

- F.-X. Dupe, A. Rassat, J.-L. Starck, M. J. Fadili , "An Optimal Approach for Measuring the Integrated Sachs-Wolfe Effect", arXiv:1010.2192, *Astronomy and Astrophysics*, 534, A51+, 2011.

- Sparse-Inpainting preserves the large scales anomalies

- A. Rassat and J-L. Starck, "On Preferred Axes in WMAP Cosmic Microwave Background Data after Subtraction of the Integrated Sachs-Wolfe Effect", Astronomy and Astrophysics , 557, id.L1, pp 7, 2013.
- A. Rassat, J-L. Starck, and F.X. Dupe, "Removal of two large scale Cosmic Microwave Background anomalies after subtraction of the Integrated Sachs Wolfe effect", Astronomy and Astrophysics , 557, id.A32, pp 15, 2013.

Generalized MCA (GMCA)

•J. Bobin, J.-L. Starck, M.J. Fadili, and Y. Moudden, "Sparsity, Morphological Diversity and Blind Source Separation", IEEE Trans. on Image Processing, Vol 16, No 11, pp 2662 - 2674, 2007.
•J. Bobin, J.-L. Starck, M.J. Fadili, and Y. Moudden, "Blind Source Separation: The Sparsity Revolution", Advances in Imaging and Electron Physics , Vol 152, pp 221 -- 306, 2008.

Source: $S = [s_1, \ldots, s_n]$ Data: $X = [x_1, \ldots, x_m] = AS$

We now assume that the sources are linear combinations of morphological components :

$$s_i = \sum_{k=1}^{K} c_{i,k} \quad \text{such that} \quad \alpha_{i,k} = T_{i,k} c_{i,k} \text{ sparse}$$

$$\Longrightarrow \quad X_l = \sum_{i=1}^{n} A_{i,l} s_i = \sum_{i=1}^{n} A_{i,l} \sum_{k=1}^{K} c_{i,k}$$

==> GMCA searches a sparse solution S in the dictionary ϕ subject to the constraint that the norm $\| X - AS \|^2$ is minimal.

$$\phi = [[\phi_{1,1}, \ldots, \phi_{1,K}], \ldots, [\phi_{n,1}, \ldots, \phi_{n,K}],], \quad \alpha = S\phi^t = [[\alpha_{1,1}, \ldots, \alpha_{1,K}], \ldots, [\alpha_{n,1}, \ldots, \alpha_{n,K}]]$$

GMCA aims at solving the following minimization:

$$\min_{A, c_{1,1}, \ldots, c_{1,K}, \ldots, c_{n,1}, \ldots, c_{n,K}} = \sum_{l=1}^{m} \left\| X_l - \sum_{i=1}^{n} A_{i,l} \sum_{k=1}^{K} c_{i,k} \right\|_2^2 + \lambda \sum_{i=1}^{n} \sum_{k=1}^{K} \| T_{i,k} c_{i,k} \|_p$$

Sparse Component Separation: the GMCA Method

A and S are estimated alternately and iteratively in two steps :

1) Estimate S assuming A is fixed (iterative thresholding) :

$$\{S\} = \mathrm{Argmin}_S \sum_j \lambda_j \|s_j \mathbf{W}\|_1 + \|\mathbf{X} - \mathbf{AS}\|^2_{F,\boldsymbol{\Sigma}}$$

2) Estimate A assuming S is fixed (a simple least square problem) :

$$\{A\} = \mathrm{Argmin}_A \|\mathbf{X} - \mathbf{AS}\|^2_{F,\boldsymbol{\Sigma}}$$

BSS experiment : Noiseless case

Original Sources




2 of 4 Mixtures


Noiseless experiment, 4 random mixtures, 4 sources

GMCA Experiment

•J. Bobin, J.-L. Starck, M.J. Fadili, and Y. Moudden, "Sparsity, Morphological Diversity and Blind Source Separation", IEEE Trans. on Image Processing, Vol 16, No 11, pp 2662 - 2674, 2007.